

## Infrared active modes in large clusters of spheres\*

M. Ausloos<sup>†</sup> and P. Clippe

*Institut de Physique, B5, Université de Liège, B-4000, Sart Tilman/Liège 1, Belgium*

A. A. Lucas

*Département de Physique II, Facultés Universitaires, Notre Dame de la Paix B-5000 Namur, Belgium*

(Received 14 March 1977)

Some previous work on the effect of aggregation on the infrared absorption spectrum of small-dielectric-sphere powders is extended in order to take into account various cluster sizes and shapes. A model recently introduced is critically discussed. Trends are given for the spectral bounds, the largest absorption strengths, and the possible structure in an infrared powder spectrum, as a function of the number of crystallites. Application of our results to NiO powder spectrum is briefly made. According to our calculation, the upper half of the spectrum can be completely covered by modes belonging to the considered clusters. The assumption that crystallites are spheres is discussed. One conclusion is that it is necessary to go beyond the approximation of identical ionic crystal spheres if a powder spectrum has to be interpreted.

PACS numbers: 78.20.Dj, 78.30.-i, 78.50.-w

### I. INTRODUCTION

In a recent paper, Clippe *et al.* (CEL) have briefly summarized various theoretical approaches to describe the broadening of the infrared (ir) spectrum of powders with respect to that predicted for bulk systems.<sup>1</sup> They have discussed another broadening mechanism, the clumping effect, which takes into account the clusterlike consistency of powders. This physical picture is, in fact, closer to reality. In addition, their work involves several theoretical approximations, which are clearly stated in their paper. Some of these assumptions are studied here.

The physical model of CEL consists of identical ionic spheres, forming small clusters. Within the clusters, the particles interact via the dipolar interaction without any retardation effect. The ir-active modes of clusters containing a few particles (pair, linear triplet, linear quadruplet, tetrahedron) have been reported in Ref. 1. The long wavelength dipolar-active modes of the infinite linear chain, the infinite double-strand chain, the close-packed planar cluster, and the three-dimensional fcc lattice have also been given. For the first four (finite) clusters, the eigenvectors (which are needed to calculate the total dipole moment) have also been calculated and reported. CEL theory is briefly recalled in Sec. II in order to introduce the notation.

The ir spectrum of powders is analyzed using the bulk material ir spectrum as a reference. The bulk transverse-optical and longitudinal-optical mode frequencies are, respectively,  $\omega_T$  and  $\omega_L$ . It is generally observed that the ir spectrum of powders spans the frequency range  $[\omega_T, \omega_L]$  and presents some weak structure depending on the powder preparation. CEL have applied their the-

ory to NiO powders. In such a case, the frequencies of ir-active modes calculated for the above list of eight clusters cover 70% of the interval ( $\omega_T = 401 \text{ cm}^{-1}$ ,  $\omega_L = 598 \text{ cm}^{-1}$ ).

However infinite clusters are quite unlikely. If modes due to such clusters are not considered, the range covered by the ir-active modes of the finite clusters covers only about 27% of the interval  $[\omega_T, \omega_L]$ , and surprisingly the lower half of the interval is not covered at all. However, the ir absorption spectrum of NiO powders prepared from commercially available powder has a broad peak<sup>2</sup> (above a large continuum) below  $500 \text{ cm}^{-1}$ , i.e.,  $\frac{1}{2}(\omega_T + \omega_L)$ .

Thus, such a peak does not correspond to any frequency calculated by CEL. For completeness, let us recall that ir extinction coefficient for NiO smoke in air has more structure,<sup>2</sup> also unexplainable from the CEL set of predicted ir active modes.

In their conclusion, CEL suggest that other cluster geometries be investigated. Only geometrical effects have indeed to be considered as we shall discuss in Sec. II A (and Appendix A). Application of the theory to specific powders can later be made through Eq. (17) of CEL or Eq. (A1).

In Sec. II B, much more complex clusters than those considered by CEL are investigated. They contain up to 24 spheres. Only results pertaining to experimentally observable effects are reported here. In such a respect, some attention is centered on four different points (i) the low-frequency region of the spectrum, (ii) the upper edge of the ir-absorption active modes, (iii) therefore the cluster spectral bounds, and (iv) the largest "absorption strength." The latter is defined in Sec. II.

The ir-absorption active modes are not easily

characterized in terms of symmetry properties of the cluster. In particular "edgelike" and "cornerlike" effects appear in irregularly shaped clusters.

Section III contains a discussion of our results. It is observed that a more or less compact cluster will have a different type of ir absorption spectrum. However, the spectral bounds of the large finite clusters which we have considered all fall within the frequency range of the peculiar infinite extent clusters examined by CEL.

Hence, the upper (lower) half of the spectrum can (cannot) be described in the framework of the previous CEL theory. The peak near  $500 \text{ cm}^{-1}$  is here not definitively attributed to a specific cluster although one can consider that it is due to irregular very long chains. Several suggestions for modifying the "all identical sphere clumping" model are presented. Broadening mechanisms other than the clumping effect are suggested.

## II. ir SPECTRUM OF DIPOLAR CLUSTERS

### A. Theory

CEL aims at obtaining the frequency spectrum of a cluster of identical ionic crystal spheres from the overlap between the electric field of each sphere considered as an oscillating dipole. The frequencies of the collective oscillations are calculated by diagonalizing a  $3N$  by  $3N$  matrix, where  $N$  is the number of spheres in a given cluster.

Let  $i$  and  $j$  label two different spheres in the cluster,  $\sigma$  and  $\nu$  label Cartesian components of a vector,  $R$  be the radius of a sphere,  $R_{ij}$  be the distance between centers of spheres  $i$  and  $j$ ,  $\hat{R}_{ij}^0$  be the corresponding unit vector,  $\hat{R}_{ij}^0 \otimes \hat{R}_{ij}^0$  be the dyadic obtained from the direct product of  $\hat{R}_{ij}^0$  with itself, i.e., a matrix for which the  $\sigma\nu$  element is  $R_{ij}^{\sigma\nu} R_{ij}^{\sigma\nu}$ , and  $\underline{1}_{\sigma\nu}$  be the unit matrix.

The matrix to be diagonalized is

$$\underline{T}_{3N} \equiv \begin{bmatrix} 0 & T_{12} & T_{13} & \cdots & T_{1N} \\ T_{21} & 0 & \cdots & \cdots & \\ T_{31} & T_{32} & 0 & T_{3j} & \vdots \\ \vdots & T_{ji} & & \ddots & \\ T_{N1} & \vdots & \cdots & & 0 \end{bmatrix}, \quad (1)$$

where the  $3 \times 3$  matrices  $T_{ij}$  have elements

$$T_{ij}^{\sigma\nu} = (\underline{1}_{\sigma\nu} - 3R_{ij}^{\sigma\nu} R_{ij}^{\sigma\nu}) / R_{ij} / R^3. \quad (2)$$

Notice that  $T_{ij}$  is a diagonal matrix, only if the sphere centers form a linear chain. The magnitude of the dipole moment of a single sphere is equal to unity.

Let  $\lambda_\mu$  be any of the eigenvalues of  $T_{3N}$ , and  $\tilde{x}_i^\mu$ ,  $i=1, \dots, N$  the corresponding eigenvectors. It is clear that  $\lambda_\mu$  is a purely geometrical factor which depends only on the geometry of spheres within a cluster, and not on the material. CEL show that one has  $-1 \leq \lambda_\mu \leq 2$ . By convention, the eigenvalues are ordered in such a way that  $\lambda_1 \geq \lambda_2 \geq \dots \geq \lambda_{3N}$ . From such a set of  $\lambda_\mu$ , one can obtain readily the ir active modes  $\omega_\mu$  of the powder, when the static  $\epsilon_0$  and high-frequency  $\epsilon_\infty$  dielectric constants of the bulk material are known, along with the value of the Fröhlich surface mode  $\omega_s$  and the dynamic polarizability of one ionic sphere [Eq. (17) in CEL].

Finally, let  $\{\tilde{x}_i^\mu\}$ , with  $i=1, \dots, N$ , be the set of oscillation vectors of the  $1, \dots, N$  spheres, corresponding to the mode  $\mu$  (or "eigenshift"  $\lambda_\mu$ ). The absorption strength due to the mode  $\mu$  is defined by

$$A^\mu = \left( \sum_{i=1}^N \tilde{x}_i^\mu \right)^2 \quad (3)$$

under the assumptions discussed by CEL.

The eigenvectors  $\tilde{x}_i^\mu$  themselves are *not meaningful* quantities when eigenvalues are degenerate. In such a case, eigenvectors depend on the sphere labeling within a cluster. Only  $A^\mu$  is invariant with respect to such a permutation of sphere labels and is a meaningful quantity. Hence eigenvectors are not drawn nor reported here.

### B. Results

A complete list of eigenvalues and eigenvectors is available from the authors. It is only useful to report those eigenvalues  $\lambda_\mu$  for which the absorption strength  $A^\mu \neq 0$ . Furthermore, several ir-active modes of a cluster can have a very small absorption strength. Their observation is unlikely except if such a cluster is highly probable in a powder. Not much information is available on cluster size, shape, and statistics in powders. Hence it seems appropriate to quote only which negative and which positive eigenvalue has the largest  $A^\mu$ .

Since CEL found ir-active modes in the upper frequency part of the powder spectrum, but a smooth central peak is observed, some emphasis must be placed on the most negative eigenvalue. However, the most positive eigenvalue will be reported as well for completeness. In experimental work such most positive eigenvalues could, in fact, be the most easily identified.

The absorption strength corresponding to the spectral bounds will be also given. Such  $A^\mu$  can, however, be very small.

In order to characterize the spectrum and the

mode distribution, other numbers are of interest. Since eigenvalues can be degenerate, their multiplicity  $m$  will be given.

The number  $M$  of different  $\lambda^\mu$ 's which have a nonzero  $A^\mu$  is a relevant quantity. It is a measure of the spectrum density. These  $M$  eigenvalues are numbered by an index  $p$  (such that  $\lambda_1 > \lambda_p > \lambda_\mu$ ), which indicates the relative position of the interesting eigenvalue with respect to the extreme values for a cluster.

One-, two-, and three-dimensional systems of touching spheres are successively examined, arranged according to the number of particles in a cluster and the cluster complexity or lack of symmetry. For the sake of clarity only the centers of the spheres are indicated by black dots. In the following tables, only representative clusters are taken into account. The figures contain more data, though in a more condensed way.

Results due to CEL are not reported, although in Ref. 1, a few misprints are corrected.

### 1. Linear clusters

This class of clusters contains linear single-strand chains (Table I). The smallest eigenvalue is always  $\lambda_{3N}$ , and always corresponds to the max-

TABLE I. Characteristic eigenvalues  $\lambda_\mu$  and corresponding absorption strength  $A^\mu$  for spherical crystallites forming a perfect linear chain. Other symbols ( $p$  and  $m$ ) are explained in Sec. II B.

$N$	$M$	$p$	$\mu(m)$	$\lambda_\mu$	$A^\mu$
2	2	1	2(2)	0.125	2
		2	6	-0.25	2
3	4	1	1	0.338	0.065
		2	2(2)	0.185	2.935
		4	9	-0.369	2.935
4	4	1	2(2)	0.218	3.839
		4	12	-0.435	3.839
5	6	1	1	0.401	0.0172
		2	3(2)	0.238	4.725
		5	12(2)	-0.201	0.0172
		6	15	-0.476	4.725
6	6	1	2	0.309	0.0477
		2	3(2)	0.251	5.6002
		6	18	-0.502	5.6002
7	8	1	1	0.423	0.0069
		2	3(2)	0.261	6.468
		8	21	-0.522	6.468
12	12	1	2	0.410	0.0064
		3	5(2)	0.282	10.745
		12	36	-0.565	10.745
15	16	1	1	0.444	0.0008
		3	5(2)	0.288	13.286
16	16	16	45	-0.575	13.286
		1	2	0.427	0.0028
		3	6(2)	0.289	14.131
		16	48	-0.577	14.131

imum  $A^\mu$ . For  $N$  even (odd), one has  $M=N$  ( $M=N+1$ ). Absorption strength of the spectral upper bound is always very small.

### 2. Planar clusters

a. Double- and triple-strand perfect chains. Such systems already contain some edge and cor-

TABLE II(a). Same as in Table I, but for spherical crystallites forming a perfect double-strand planar chain. (b) Same as in Table I, but for spherical crystallites forming a perfect triple-strand planar chain.

$N$	$M$	$p$	$\mu(m)$	$\lambda_\mu$	$A_\mu$
(a)					
4	3	1	3	0.294	4
		3	8(2)	-0.164	3.767
6	8	1	1	0.501	0.0784
		2	3	0.235	5.880
		7	16	-0.294	5.753
		8	17	-0.399	0.0389
8	10	1	3	0.426	7.701
		9	21	-0.371	7.595
		10	22	-0.382	0.0095
12	15	1	3	0.482	0.0385
		2	4	0.476	11.255
		15	35	-0.452	11.174
16	20	1	3	0.525	0.0237
		2	4	0.500	14.744
		19	46	-0.492	14.683
		20	47	-0.508	0.0089
20	25	1	3	0.548	0.0137
		3	5	0.515	18.198
		24	58	-0.516	18.156
		25	59	-0.542	0.0060
		22	29	1	1
		3	5	0.520	19.915
		28	64	-0.524	19.884
		29	65	-0.554	0.0049
(b)					
9	8	1	1(2)	0.561	0.129
		2	3	0.476	8.660
		6	21(2)	-0.263	8.056
12	16	8	26(2)	-0.490	0.057
		1	2	0.592	0.1715
		2	3	0.532	11.360
15	22	14	32	-0.339	11.041
		16	36	-0.536	0.0728
		1	1	0.618	0.034
		3	3	0.568	14.012
18	24	19	39	-0.390	13.827
		22	45	-0.563	0.092
		1	2	0.621	0.255
		2	3	0.593	16.633
21	30	21	47	-0.425	16.528
		24	54	-0.579	0.114
		1	1	0.637	0.0138
		3	3	0.610	19.231
		26	56	-0.450	19.184
		30	63	-0.590	0.1401

ner effects. The maximum absorption strength usually does not correspond to the minimum eigenvalue [Tables II(a), and II(b)]. Absorption strengths of the extremum ir-active modes are always very small, except for the  $2 \times 4$  and  $2 \times 6$  planar configuration.

b. Irregular planar chains. It is always assumed that the center of each sphere is located on a site of a regular square lattice. This restriction could be removed in further work, but does not seem of great importance here.

Planar (single, double, triple, ...) strand chains can have various "defects" (planar steps and other dislocationlike structures) leading to asymmetric distributions of eigenvalues. Table III contains representative chains with various defects. Due to the lack of symmetry in such systems, the number  $M$  of ir-active modes is close to the number of degrees of freedom ( $3N$ ) of the cluster. The maximum absorption strength always corresponds to a positive shift.

### 3. Three-dimensional arrays

Single- and double-strand chainlike systems which contain edges and corners have been studied, along with other "bizarre" clusters. A few representative systems are displayed in Table IV

TABLE III. Same as in Table I, but for spherical crystallites forming a disordered connected planar cluster. Black dots represent the crystallite centers sitting on a square-planar lattice.

	N	M	p	$\mu$ (m)	$\lambda_{\mu}$	$A^{\mu}$
	4	12	1	1	0.368	0.224
			3	3	0.234	3.869
			12	12	-0.388	2.393
	4	11	1	1	0.374	0.012
			3	3	0.254	3.865
			11	12	-0.382	2.219
	4	6	2	3	0.343	0.078
			5	10	0.247	3.896
			6	12	-0.227	3.054
					-0.306	1.515
	5	13	1	1	0.376	0.2896
			3	3	0.266	4.847
			12	14	-0.278	1.825
			13	15	-0.404	1.841
	5	5	1	1(2)	0.404	0.1499
			2	3	0.307	4.764
			5	14(2)	-0.391	1.735
	5	13	1	1	0.387	0.348
			3	3	0.257	4.735
			12	14	-0.334	2.548
			13	15	-0.418	2.525
	5	15	5	1	0.404	0.0691
			3	3	0.275	4.708
			15	15	-0.442	3.316
	5	13	1	1	0.370	0.0028
			3	3	0.277	4.806
			11	13	-0.303	3.468
			13	15	-0.315	0.0049
	6	9	1	1	0.389	0.2486
			2	4	0.283	5.5752
			9	18	-0.398	5.2797
	16	48	1	1	0.444	0.0045
			6	6	0.291	14.496
			8	48	-0.576	13.321
	16	11	1	3	0.595	14.919
			9	38(2)	-0.318	7.621
			11	45 2	-0.513	0.1058

for  $N \leq 16$ . The maximum absorption strength can lie either in the upper or the lower part of the eigenvalue spectrum.

Cluster modes of cubic basic units are also of interest. In addition to their theoretical simplicity they could be present in powders formed from cubic materials after cutting and grinding. Table V contains representative values for chains of simple cubic units. A chain of two fcc units has been also considered as well as a 22-particle cluster made of a perfect chain of three fcc units without external faces.

Except for the chain of one and two fcc units, the largest absorption strength corresponds to a negative eigenvalue. In the case of single cubic unit chains, the spectral bounds correspond to extremely small absorption strengths. The results presented in Tables I-V are reported on Figs. 1-4, along with information pertaining to all the other clusters which we have examined. The symbols necessary to interpret the figures are explained in the Fig. 1 caption.

### III. DISCUSSION

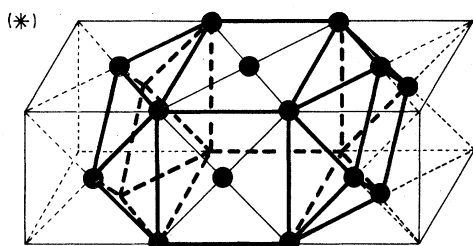
In this section, only trends are discussed. As long as further detailed experimental results are not available, many of the numerical values are

TABLE IV. Same as in Table III, but when spherical crystallite centers sit on a three-dimensional cubic lattice.

	N	M	p	$\mu$ (m)	$\lambda_{\mu}$	$A^{\mu}$
	4	12	1	1	0.376	0.1760
			4	4	0.129	2.6159
			11	11	-0.267	1.0513
			12	12	-0.328	1.0057
	4	7	1	1	0.393	0.3776
			3	4	0.088	3.000
			7	7(2)	-0.077	1.790
			7	1(2)	-0.317	0.7807
	5	15	1	1	0.504	0.0959
			5	5	0.152	2.2999
			8	8	-0.026	2.508
			15	15	-0.420	0.0003
	6	15	1	1	0.557	0.0771
			4	5	0.227	2.472
			8	9	-0.039	5.053
			15	17	-0.332	0.2818
	7	3	1	1(3)	0.479	0.966
			2	8(3)	0	4.894
			3	19(3)	-0.406	1.139
	8	12	1	2	0.540	0.244
			3	6	0.221	5.107
			7	13	-0.089	5.986
			12	23	-0.419	0.004
	8	19	1	1	0.597	0.315
			9	10	0.033	5.338
			15	18	-0.230	6.0787
			19	24	-0.483	0.8664
	9	22	1	1	0.621	0.485
			5	6	0.302	4.075
			19	22	-0.263	5.031
			22	27	-0.497	0.028
	12	18	1	2	0.564	0.558
			3	6	0.372	9.177
			16	31	-0.335	10.095
			18	35	-0.483	0.0004
	16	24	1	2	0.579	0.3167
			11	22	0.0062	12.223
			23	45	-0.411	14.295
			24	47	-0.526	0.0015

TABLE V. Same as in Table IV, but for crystallites forming a cluster with axial fourfold symmetry ( $D_4$ ). Crystallites are perfectly aligned along a tetragonal axis.

	N	M	P	$\mu$ (m)	$\lambda_\mu$	$A^\mu$
cube	8	2	1	4 (3)	0.302	1.214
			2	13 (3)	-0.054	6.786
bcc	9	3	1	1 (3)	0.594	0.8858
			2	13 (3)	0	6.8986
			3	25 (3)	-0.433	1.216
fcc	14	4	1	5 (3)	0.683	0.6632
			2	13 (3)	0.210	7.125
			3	26 (3)	-0.233	2.458
			4	29 (3)	-0.367	3.754
3 sc units	16	10	1	3	0.717	0.00009
			2	19 (2)	0.091	7.982
			3	35	-0.281	14.887
			4	36 (2)	-0.343	0.0109
4 sc units	20	13	1	2	0.767	$75 \times 10^{-5}$
			2	21 (2)	0.110	7.469
			3	45	-0.3395	18.573
			4	49 (2)	-0.384	0.0009
See (*)	22	15	1	2	0.967	0.1464
			2	25 (2)	0.0196	11.382
			3	35	-0.160	14.275
			4	62 (2)	-0.548	0.0942
2 fcc	23	17	1	2	1.058	0.0588
			2	17 (2)	0.300	8.758
			3	41 (2)	-0.237	8.0445
			4	65 (2)	-0.550	0.1062



not needed. It is in fact necessary to know powder statistics before explicitly analyzing a given spectrum.

We will examine successively: general trends as a function of  $N$ , general trends for the absorption strength, general trends for the eigenvalues.

From Figs. 1–4, a few interesting points can be noticed.

(a) The maximum and minimum eigenvalues increase monotonically in magnitude with the number of atoms. The rate of increase depends on the cluster configuration.

(b) The maximum absorption strength increases with the number of atoms.

(c) In the case of planar systems, the largest absorption strength always corresponds to a positive eigenvalue, except in the case of linear chains.

(d) In the case of linear chains, the absorption strength has two equal maxima. One maximum always corresponds to the most negative eigenvalue. That corresponding to a positive eigenvalue moves toward the center of the spectrum as  $N$  increases.

(e) In the case of three-dimensional clusters, the maximum absorption strength often corresponds to a negative eigenvalue (except for systems with  $O_h$  symmetry, where it corresponds to zero eigenvalue).

(f) For  $N \leq 18$ , the smallest eigenvalue is always that of the linear chain.

(g) For a given  $N$ , the smallest eigenvalue of the double-strand chain is always smaller than

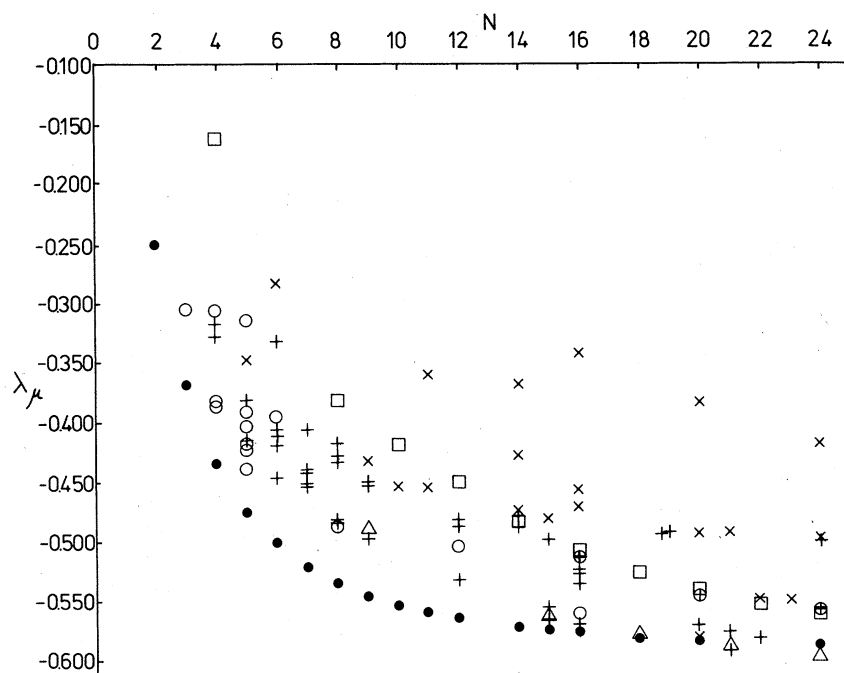


FIG. 1. Variation of the smallest eigenvalue of ir-active modes for various clusters according to the number  $N$  of crystallites in a cluster. Symbols are as follows: ● systems defined in Table I as perfect linear chains; □ systems defined in Table II(a) as perfect double-strand chains; △ systems defined in Table II(b) as perfect triple-strand chains; ⊕ systems forming a perfect quadruple-strand chain; ○ systems defined in Table III as planar clusters; + systems defined in Table IV; X systems defined in Table V.

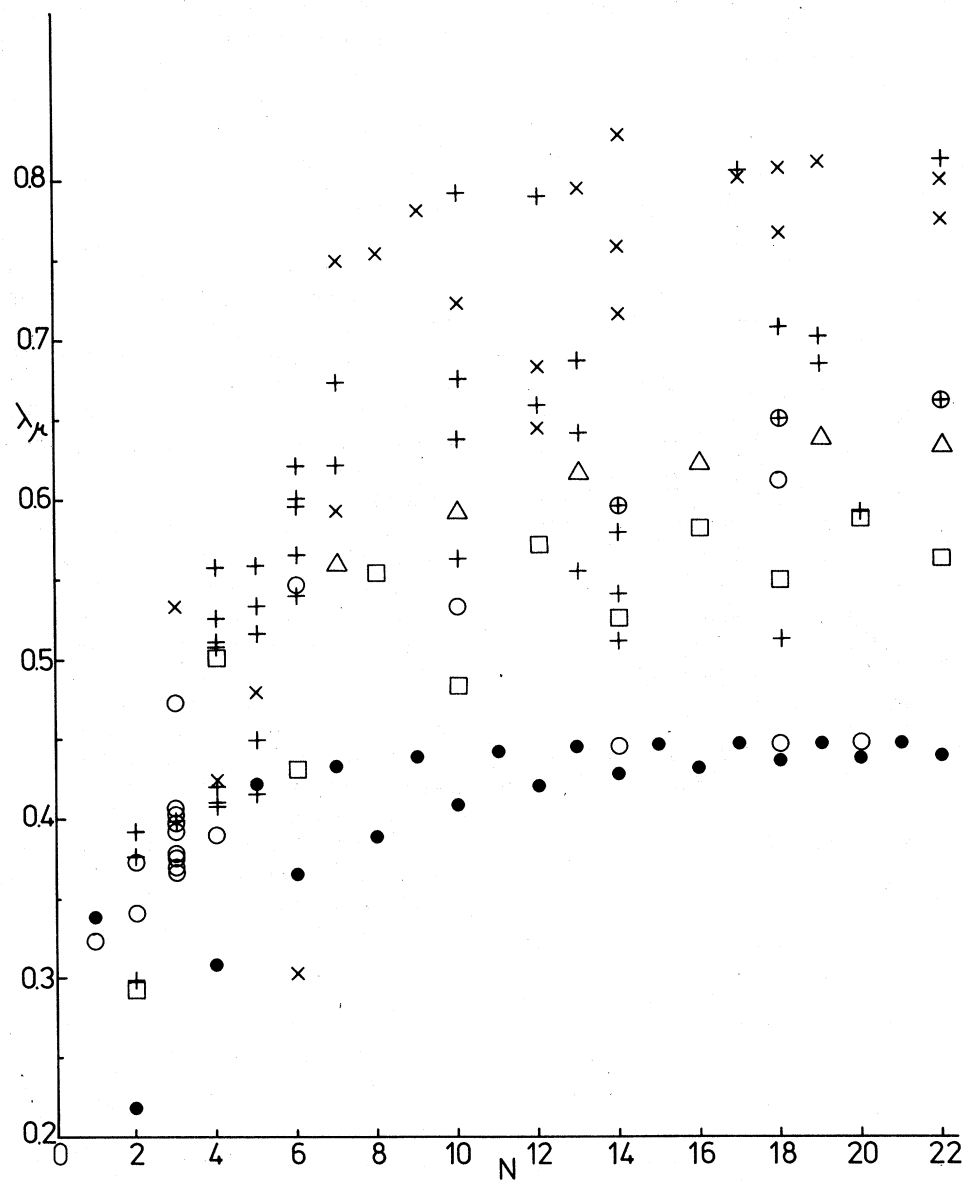


FIG. 2. Variation of the largest eigenvalue of ir-active modes for various clusters according to the number  $N$  of crystallites in a cluster. Symbols are explained in caption of Fig. 1.

the smallest eigenvalue for a linear chain.

(h) For  $N > 18$ , the smallest eigenvalue is that of the perfect triple-strand chain.

(i) For  $N < 24$ , the smallest eigenvalue always corresponds to a planar configuration.

(j) It is conjectured that  $N$  must be quite large before a three-dimensional configuration will have the smallest eigenvalue. Indeed, CEL have indicated that the infinite three-dimensional fcc lattice seems to have the smallest eigenvalue ( $\sim -0.630$ ), but is quite close to the smallest eigenvalue for a linear chain ( $\sim -0.601$ ).

(k) However, in the case of clusters made of aligned fcc units the largest absorption strength corresponds to a positive eigenvalue.

(l) For a given  $N$ , the most negative eigenvalue tends to be larger in magnitude for less compact systems.

(m) For a given  $N$ , the largest absorption strength corresponding to a negative eigenvalue is in general that of the more compact system.

(n) A noticeable exception to (m) is that of clusters made of fcc units, for which the largest absorption strength is quite small in comparison to

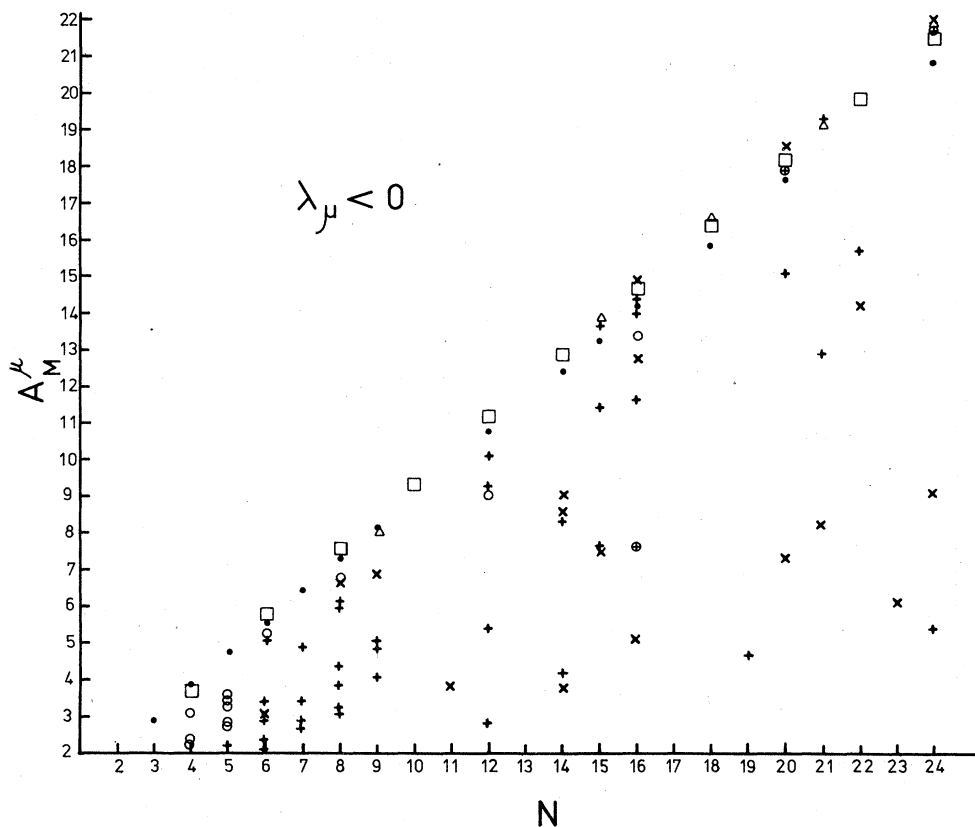


FIG. 3. Largest absorption strength corresponding to a negative eigenvalue  $\lambda_\mu$  for various clusters, as a function of the number  $N$  of crystallites in a cluster. Symbols are explained in Fig. 1 caption.

that of planar systems and has an eigenvalue  $\lambda$  close to zero.

(o) For a given  $N$ , the largest absorption strength corresponding to a positive eigenvalue is that of the most compact planar system.

(p) The most positive eigenvalue corresponds to the most compact system for a given  $N$ .

(q) For a given  $N$ , the largest absorption strength is very close to that of the one-strand linear chain.

From statements (h)–(j) in particular, it appears that the  $N \rightarrow \infty$  cluster considered by CEL gives the true theoretical limits for the ir spectrum of their model powder. In Appendix A, we indicate that it is sufficient to discuss the spectrum in terms of the set of universal parameters  $\lambda_\mu$ .

However, one can estimate the frequency range which is predicted for a few clusters and give a few frequencies corresponding to large absorption strength in the case of a typical powder, like NiO. In Table VI, the results of an application of formula (17) of CEL to the above data are reported.

(Material characteristics are given in Appendix A).

The NiO powder spectrum<sup>2</sup> which could be covered by the frequency range predicted along the CEL model is presented on Fig. 5. The extreme ir-active modes are at 503 and 585  $\text{cm}^{-1}$  for the  $N < 24$  clusters which we have considered, and for the  $\epsilon_0, \epsilon_\infty$  and (Fröhlich mode)  $\omega_s$  values given in Appendix A for NiO.

Powder pictures usually show clusters which are either compact globules or long chains with  $N$  finite ( $N < 30$  on pictures which we have seen).<sup>2</sup> The above range of frequencies could be somewhat modified if the values of  $\epsilon_0, \epsilon_\infty$ , and  $\omega_s$  are slightly modified. Indeed bulk values are used here.

However, it seems difficult to reproduce the complete absorption spectrum from CEL model and its extension. Even the  $N = 24$  linear chain lower ir-active absorption mode is situated above 500  $\text{cm}^{-1}$ . Therefore the broad peak at 500  $\text{cm}^{-1}$  can only be cautiously attributed to the presence of very long, most likely somewhat irregular, chains.

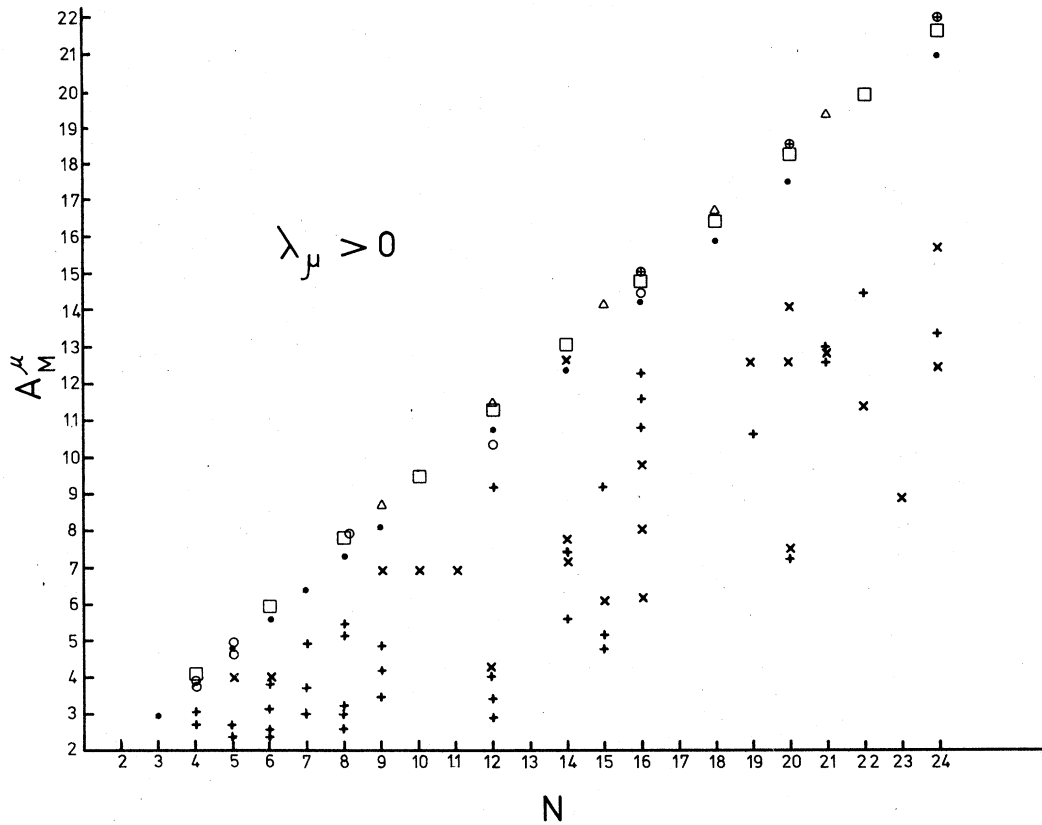


FIG. 4. Largest absorption strength corresponding to a positive eigenvalue  $\lambda_\mu$  for various clusters, as a function of the number  $N$  of crystallites in a cluster. Symbols are explained in Fig. 1 caption.

According to our analysis and some "delicate" intuition, several approximations in our model can be challenged.

(i) Powder spheres do *not* need to be *identical*. Since the sphere radius enters as a scaling factor in Eq. (2), it is easy to generalize such an equation in order to take into account a distribution of radii. Although the Fröhlich surface mode  $\omega_s$  is radius independent, collective oscillations will depend on radius distribution.

(ii) Similarly, powder spheres do not need to have all the same dipolar moments. In fact a scaling relation holds; since the dipole moment of a sphere is proportional to its volume, only

the factor  $p_i D_i^3$  has to be considered as a random number, where  $D_i$  is the diameter of the sphere containing a dipole  $p_i$ . A random distribution of dipolar moments will be considered in future work.

(iii) Powder components do *not* need to be *spheres*. Indeed, independent work on single cubes and rectangular parallelepipeds has indicated the need to consider edge and corner effects.<sup>3</sup> In cubes, modes corresponding to the single Fröhlich mode of a sphere have been calculated. Their position depends on  $\epsilon(\omega)$  also. It was found that only a few modes have rather large dipolar nature. They are spread over the whole  $(\omega_T, \omega_L)$  range, the extreme modes having the greatest strength. Some mode accumulation with small strength occurs near  $\lambda \sim 0$ . In fact, not too anisotropic parallelepipeds favor an eigenvalue close to zero.

It would be of great interest to look for collective modes of an assembly of cubes or parallelepipeds. However, some complication arises because the cube modes have various strengths in contrast to the *single* mode with large strength of a sphere. One might first search whether faces

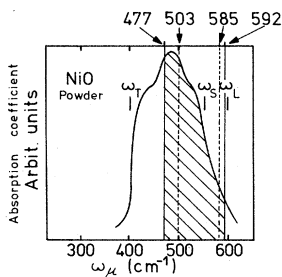


FIG. 5. ir absorption spectrum of NiO powder from Ref. 2. Shaded area corresponds to frequency range covered by results in Ref. 1 and present work. Dashed lines correspond to extreme calculated frequencies for clusters with  $N < 24$  in Sec. II.



TABLE VI. Representative frequencies of ir-active modes for a NiO powder as obtained from Eq. (A1) and from results of Tables I-V. Symbols are those of Tables I-V. Although  $N$  and  $M$  are not sufficient to define uniquely a cluster, exact correspondence exists here between Tables I-V and this Table.

Cluster	$p$	ir absorption frequency range ( $\text{cm}^{-1}$ )	ir modes with largest $A^\mu$ ( $\text{cm}^{-1}$ )	$p$
$N=8, M=12$	1	573.17	562.21	3
	12	521.72	543.68	7
bcc unit $N=9$	1	574.68	552.00	2
	3	520.37		
$N=9, M=22$	1	575.42	565.33	5
	22	513.46	535.33	19
Linear chain $N=11$	1	570.06	564.52	3
	17	505.81	505.81	17
$N=12, M=18$	1	573.83	567.84	3
	18	514.99	529.48	16
Linear chain $N=16$	1	569.67	564.86	3
	16	503.43	503.43	16
Double-strand chain $N=16$	1	572.71	571.98	2
	20	512.11	513.98	19
$N=16, M=24$	1	574.28	552.32	11
	24	510.09	522.52	23
Planar rectangle $N=20$	1	576.19	575.79	3
	26	507.48	526.05	22
2 fcc unit $N=23$	1	585.26	565.28	5
	17	507.04	537.21	10
Linear chain $N=24$	1	570.09	565.06	4
	24	501.93	501.93	24
Triple-strand chain $N=24$	1	575.77	575.48	2
			543.65	21
	32	500.75	516.49	29

or edges have simple dipolar modes, say  $\Omega_s$ , then apply Eq. (17) of CEL, or Eq. (A1).

(iv) More generally, other geometrics are possible.<sup>2</sup> Work on small ionic cluster and metallic clusters has indicated the peculiar fivefold symmetry of such systems.<sup>4</sup> They are characterized by a large amount of edges and corners with respect to a given surface and volume.

(v) An interaction similar to that between electrons in a polarizable medium can also take place between fluctuating dipoles. This indirect interaction has been recently considered.<sup>5</sup>

(vi) Cluster-cluster interactions can also lead to some spectrum broadening, as it will be shown elsewhere.

(vii) Finally, higher-order multipolar interaction could be considered.

In conclusion, it seems evident that the present work has given some insight toward describing

some ir spectrum powder broadening, although it falls short of fully explaining a given powder spectrum. Much more work is still necessary before a powder spectrum can be easily and completely interpreted.

#### APPENDIX A

According to Ref. 1, the ir active modes  $\omega_\mu$  are given by

$$\omega_\mu = \omega_s \left( \frac{1 + \lambda_\mu (\epsilon_0 - 1) / (\epsilon_0 + 2)}{1 + \lambda_\mu (\epsilon_\infty - 1) / (\epsilon_\infty + 2)} \right)^{1/2} \quad (\text{A1})$$

where  $\omega_s$  is the Fröhlich surface mode defined by  $\epsilon(\omega_s) + 2 = 0$ , while  $\epsilon_0$  and  $\epsilon_\infty$  are the static and high-frequency dielectric constants of the bulk material.

Consider the typical case of NiO powders for which  $\omega_s = 552 \text{ cm}^{-1}$ ,  $\epsilon_0 = 12$ ,  $\epsilon_\infty = 5.4$ , the above

relation becomes

$$\omega_{\mu} = \omega_s [(1 + 0.786 \lambda_{\mu}) / (1 + 0.595 \lambda_{\mu})]^{1/2}. \quad (\text{A2})$$

Since  $-1 \leq \lambda_{\mu} \leq 2$ , the relation between  $\omega_{\mu}$  and  $\lambda_{\mu}$  is in general nonlinear. Some algebra shows that the variation of  $\omega_{\mu}$  with  $\lambda_{\mu}$  is, however, monotonical in the allowed range. However, we have found here eigenvalues such that  $-0.577 \leq \lambda_{\mu} \leq 1.058$  (hence a range of  $\omega_{\mu}$  extending from  $503 \text{ cm}^{-1}$  till  $585 \text{ cm}^{-1}$ ). Hence one can approximate the above relation by

$$\omega_{\mu} \approx \omega_s (1 + 0.096 \lambda_{\mu}), \quad (\text{A3})$$

and consider that the relationship between  $\omega_{\mu}$  and  $\lambda_{\mu}$  is approximately linear in this range. Since  $\epsilon_0 > \epsilon_{\infty}$ , the latter relationship is indeed approximately valid when

$$|\lambda_{\mu}| < (\epsilon_0 + 2) / (\epsilon_0 - 1),$$

i.e.,

$$|\lambda_{\mu}| < 1.27 \text{ for NiO.}$$

Therefore it is quite sufficient for our purpose to compare our results to a specific (NiO) powder spectrum centered on  $\lambda_{\mu} \approx 0$ , in terms of the universal (geometrical) parameters  $\lambda_{\mu}$  instead of  $\omega_{\mu}$ .

\*This work has been performed in the framework of the joint project Electronic Structure in Solids (ESIS) of the University of Liege and the University of Antwerp.  
 †Also at International Center for Theoretical Solid State Physics—Belgium.

<sup>1</sup>P. Clippe, R. Evrard, and A. A. Lucas, Phys. Rev. B **14**, 1715 (1976). Notice a few misprints in tables of this reference. In Table I, line 9, instead of 2.33, read 2.23. In Table II, line 9, instead of -0.169, read 0.338; line 9, instead of 0.072, read 0.16; line 10, instead of 3.5, read 3.83; line 15, instead of 1.7, read

0.23; line 15, instead of 0.160, read 0.119; line 16, instead of -0.204, read -0.164. In Table III, line 10, instead of 539.6, read 542.3; line 11, instead of 542.0, read 566.6; line 16, instead of 559.7, read 557.8.

<sup>2</sup>A. J. Hunt, T. R. Steyer, and D. R. Huffman, Surf. Sci. **36**, 454 (1973).

<sup>3</sup>D. Langbein, J. Phys. A **9**, 627 (1976).

<sup>4</sup>T. P. Martin, Phys. Rev. B **7**, 3906 (1973).

<sup>5</sup>P. P. Schmidt and J. M. McKinley, Solid State Commun. **16**, 1161 (1975).